A Congestion-Preventing Routing and Charging Scheduling Mechanism for Electric Vehicles in Dense Urban Areas

Chenn-Jung Huang

Department of Computer Science & Information Engineering, National Dong Hwa University; 1, Sec. 2, Da Hsueh Rd. Shoufeng, Hualien 974301, Taiwan; phone: +886912796179; e-mail: cjhuang@gms.ndhu.edu.tw

Kai-Wen Hu

Department of Electrical Engineering, National Dong Hwa University; 1, Sec. 2, Da Hsueh Rd. Shoufeng, Hualien 974301, Taiwan; e-mail: drive55555@gmail.com

Hsing-Yi Ho

Department of Computer Science & Information Engineering, National Dong Hwa University; 1, Sec. 2, Da Hsueh Rd. Shoufeng, Hualien 974301, Taiwan; e-mail: hokevin678@gmail.com

Hung-Wen Chuang

Department of Computer Science & Information Engineering, National Dong Hwa University; 1, Sec. 2, Da Hsueh Rd. Shoufeng, Hualien 974301, Taiwan; e-mail: pink2xd@gmail.com

Corresponding author: cjhuang@gms.ndhu.edu.tw

Traffic congestion in metropolitan areas all over the world has become a critical issue that governments must deal with effectively. Traffic congestion during rush hours causes vehicle drivers to arrive late at their destinations, resulting in significant economic losses. Although researchers have proposed solutions to the traffic congestion problem, little research work has presented a joint route and charging planning strategy for electric vehicles (EVs) that alleviates traffic congestion problems simultaneously. Accordingly, a congestion-preventing route and

charging planning mechanism for EVs is proposed in this work to tackle the complicated route and charging optimization problems of EVs. The route and charging planning proposed in this work analyzes the information provided by EVs, the charging points, and road traffic information simultaneously, and mediates the traffic jamming by means of a route and charging reservation mechanism. Possible occurrence of traffic congestion is detected in advance and traffic regulation is carried out by allocating an elastic range to the traveling period for late-booking EVs, to avoid moving during rush hours. EV owners are also encouraged to provide rideshare services for late-booking EV users during rush hours. The simulation results reveal that the proposed work can satisfy the preferred route and charging demands of EV users and alleviate traffic congestion effectively.

KEYWORDS: Optimization, electric vehicle, route and charging planning, congestion control, machine learning.

1. Introduction

Due to recent rapid urbanization, road traffic congestion in many metropolitan areas in the world has been deteriorating for years. It is observed that the occurrence rate of traffic accidents is increased during heavy traffic periods owing to the impatience and carelessness of drivers. Meanwhile, economic losses caused by traffic congestion and its adverse impact on local city development cannot be overlooked. Although real-time and historical traffic information can be collected and utilized to great effect in the vehicle navigation systems that guide traffic navigation nowadays, traffic jams are inevitable during rush hours because large volumes of vehicles invariably overload road capacity.

Numerous efforts have been made in the past to mitigate traffic congestion plaguing metropolitan areas. One possible solution is the enhancement of existing road infrastructure, such as widening roads, increasing the number of lanes, building overpasses and underpasses, etc. However, constraints on current road infrastructure upgrades and the tremendous costs of labor and construction limit the refinement of the traffic infrastructure. Accordingly, traffic management organizations and researchers must turn to developing some other traffic control mechanisms to mitigate the traffic congestion.

A vehicle navigation system, such as Google Map, can provide a vehicle driver the fastest route to a specific destination. Although a vehicle navigation system provides drivers with options for alternative routes based on historical and real-time traffic information, this does not ease traffic congestion owing to the vast number of vehicles navigating during rush hours. Researchers have therefore also adopted adaptive traffic light control systems to coordinate the traffic flow at arterial road intersections [11-12, 14]. Nevertheless, there is still much room for the improvement of traffic light control strategies because only local traffic scheduling is typically considered, with the result that the larger scale traffic congestion problem, particularly for a whole city, is not resolved effectively.

In the recent literature, several researchers proposed vehicle navigation heuristics to tackle traffic congestion problems. Kim et al. [10] proposed a dynamic vehicle routing model under traffic congestion. A Markov decision process was formulated and approximate dynamic programming was adopted to solve the routing problem. Ahmad et al. [1] reduced traffic congestion by regulating traffic at road intersections. They claimed that their proposed algorithm can be easily implemented on low cost hardware and outperformed the existing algorithms presented in the literature. Li et al. [14] adopted a reinforcement learning-based speed control strategy at freeway recurrent bottlenecks to ease traffic congestion. Menelaou et al. [16] proposed a route reservation scheme that guides vehicles driving on an uncongested road before reaching its maximal capacity. However, the mass travel demand of vehicle drivers is not resolved effectively. Angelelli et al. [2] presented a model that minimizes the average traffic congestion over the most congested road segments. A heuristic was adopted to reduce the number of road segments considered in the model to decease the computation overhead. Cao et al. [4] presented a pheromone-based traffic management mechanism to ease traffic congestion. Roadside units collect traffic information from each vehicle and predict road congestion levels accordingly. If traffic congestion is detected, a pheromone-based vehicle rerouting mechanism is activated to direct vehicles to

take alternative routes to prevent them from encountering and adding to congestion. A vehicle rerouting system was proposed in [23] to assist vehicles in selecting uncongested road segments. Both the destination of each vehicle and local traffic information were adopted to compute a cost function during the rerouting process. Pan et al. [17] presented a real-time vehicular traffic rerouting system to mitigate the congestion problem. Each vehicle exchanges updated traffic information via ad hoc vehicular networks and participates in the computation of rerouting decisions.

In addition to the approaches mentioned above, ride-sharing mobility-on-demand (MoD) services, such as Uber and Lyft, have potential as effective solutions for solving the traffic congestion problem in many metropolitan areas owing to the ubiquity of smartphone and wireless communication technologies [9]. It is expected that car accidents, labor costs, and the greenhouse effect could be reduced if the majority of private vehicle owners turned to using on-demand mobility services. Meanwhile, it has also been shown that traffic congestion during rush hours in metropolitan areas could be alleviated effectively if routing and rebalancing policies are well organized for centrally controlled MoD service management [18].

Besides the traffic congestion problem in metropolitan areas, air pollution continues to contribute to the greenhouse effect, and urban air quality has been deteriorating in recent years as well. Electric vehicles (EVs) have been considered as a viable option to replace conventional internal combustion engine vehicles, which are dependent on fossil fuels that pollute the environment. An EV is equipped with a battery, and the state of charge (SOC) of the battery declines as the EV moves. Given the limited capacity of an EV battery, it needs to be recharged from time to time. Currently, there are three options for charging an EV, namely, plug-in charging stations [5], battery-swapping services [26], and on-road wireless charging [7]. An EV can be charged at a home/workplace if the daily usage of the EV is very limited. On the other hand, an EV with frequent daily usage or one that is used for long trip driving will have to detour to a nearby charging station to get charged if a moving EV runs short of electricity. Normally, an EV driver prefers taking the shortest path to the destination and expects to recharge the EV battery within a short period

of time. Some charging services such as fast charging stations, battery-swapping services, and on-road wireless charging can meet the demand of this type of EV driver. On the other hand, there is another group of EV drivers that will select charging options with the lowest charging cost if no specific charging preference is designated.

The route and charging planning of EVs has given rise to a new thread of research in recent years. Numerous researchers have presented heuristics to tackle the EV route and charging problem in the recent literature. To name a few, Shi et al. [19] proposed a navigation strategy to search for a fast charging station with the minimal cost function. The traffic condition and distribution system loading level are used in their mechanism to alleviate the traffic and power network congestions. Xia, et al. [25] presented a hierarchical navigation mechanism based on dynamic traffic and temperature data to mitigate the peak charging load. The upper layer, which is an optimal charging time decision, computes time slots for EV charging, while the lower layer, which is the route selection layer, determines the optimal charging routes for an EV driver. Tang et al. [22] formulated a joint optimization problem of routing and charging scheduling for an Internet EV network. A distributed routing and charging strategy was developed to allow the system operator and EVs to compute the solutions jointly. Liu et al. [15] proposed a joint charging and routing optimization model for deterministic and stochastic traffic networks. A simplified charge-control algorithm for deterministic traffic networks was presented to ease computational complexity. Sun et al. [20] proposed a traffic-distribution coordination mechanism to minimize the travel cost and energy service cost of each EV driver. An augmented Lagrangian alternating direction inexact Newton model was employed to coordinate operation of traffic and power distribution networks. A dynamic electric vehicle routing model was proposed in [3] to capture the discharging/charging pattern of an EV and minimize the service time cost. A hybrid rollout algorithm incorporating a pre-planning strategy and a rollout method was adopted to solve the routing and charging problem.

It can be seen that different charging options to fit the individual preferences of each EV driver were not considered in the above-mentioned studies. Meanwhile, the traffic congestion issue is not well ad-

dressed in the literature. Most schemes presented in research work wait until vehicle drivers have nearly arrived at congested spots before taking action to alleviate congestion, based on updated real-time congestion information. Unfortunately, such real-time congestion information offers little relief for vehicle drivers that are already stuck in traffic jams. It would be much more useful for vehicle drivers to be advised to take alternative routes or other forms of transportation in advance. In sum, an effective real-time traffic prediction and congestion prevention system not only plays a key role in the development of megacities, but also reduces the travel time of vehicle drivers.

To the best of our knowledge, little research work in the literature has presented route and charging planning for EVs that focuses on the traffic congestion prevention issue. The contribution of this paper is a novel proposal for a congestion-preventing route and charging planning mechanism for EVs. A distributed computation framework is adopted to cut down the complexity of the computation performed by the conventional centralized control mechanism. Notably, support vector regressions (SVRs) are applied to estimate the travel time of an EV at each road segment based on the historical traffic data, and a congestion control mechanism is employed to deal with the traffic jam problem caused by volatile traffic conditions in real-time. An EV first examines whether the battery has enough power to reach the destination. Then it makes route and charging reservations before the trip and keeps the real-time charging information updated after the EV moves. If an EV battery will likely experience an electricity shortage during the trip, a charging option can be chosen from among a plug-in charging station, a battery swapping station, or on-road wireless battery charging by each EV user based on her/his preset preference. For instance, if an EV user is not pressed for time and the charging cost is the major concern, the EV user will prefer to choose from among some candidate routes with the lowest price for battery charging. In contrast, the charging option with the shortest charging time would be the first choice of an EV user if he or she needs to arrive at a destination as soon as possible.

The congestion control employed in this work mediates traffic jams based on the information obtained from EVs, the charging points, and road traffic information simultaneously. The proposed mechanism detects a possible occurrence of traffic congestion in advance and regulates the traffic by allocating an elastic range to the traveling period for late-booking EVs, or by suggesting the EV user takes a rideshare service or public transportation during rush hours.

In contrast to conventional MoD services, this work also allows private vehicles to offer ridesharing services and incentivizes this through a system whereby private vehicle drivers can receive rewards from the riders. Meanwhile, no traffic control is applied to public transportation, and adaptive traffic control is applied to an EV subject to the number of riders that the EV carries. The intention of this kind of traffic control is to encourage more people to take rideshare services or public transportation during rush hours. The simulation results reveal that the proposed work can satisfy the preferred route and charging demand of EVs and solve the traffic congestion problem effectively.

The remainder of this paper is organized as follows. Section 2 presents the congestion-preventing route and charging planning mechanism for EVs. The simulation results and the conclusions are given in Sections 3 and 4, respectively.

2. The Proposed Algorithm

In this work, a distributed computation framework as shown in Figure 1 is adopted to cut down the complexity of the computation of the conventional centralized control mechanism. The whole global territory is divided into different geographical regions under a hierarchical structure. All road segments, road intersections, and charging points within a geographical region are managed by a local aggregator. As shown in the bottom middle of Figure 1, a route and charging planning method for an EV is employed to compute the route and estimate the trip time for each EV to reach a designated location based on the estimated traffic and charging information provided by the local aggregator upstream, which is in charge of the geographical region the EV is located at. The module shown in the top left of Figure 1 is adopted to provide the traffic and charging information within a time span of the EV's estimated trip time, if needed. Notably, the SVR machine learning technique is adopted to estimate traffic information here because it has been used as a powerful tool in the literature for

Figure 1

Architecture of the congestion-preventing EV route and charging planning
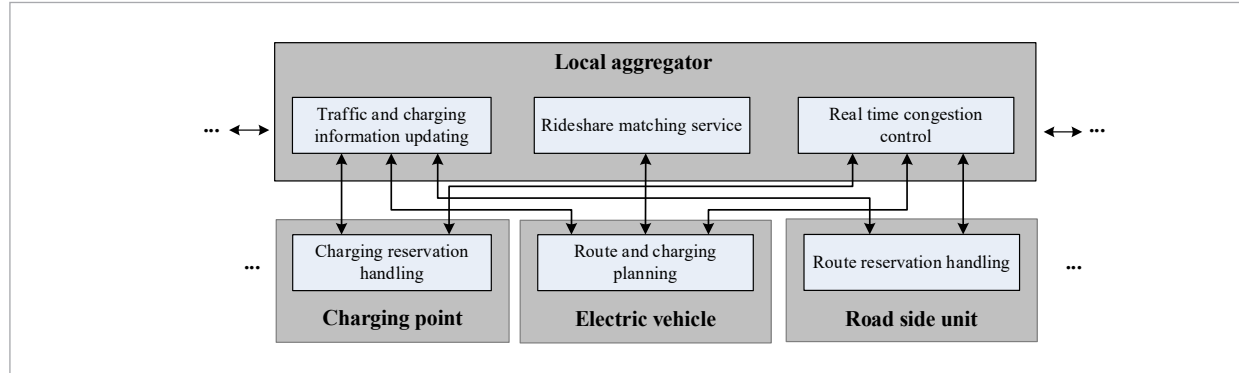
controlling processes that are difficult to model and linearize, such as the complicated traffic conditions at the road segments and intersections [24].

The EV checks if a future battery power shortage will occur before reaching the destination during the computation of the routing path. In the case of a possible battery power shortage, EV users need to select the most suitable routing paths and charging option(s) based on their preset preferences. Once an EV determines the route and charging plan that fits the preferences of passenger(s), the local aggregator upstream will receive a request from the EV for routing and charging reservations of the road segments, intersections and charging point(s) on the way from the origin to the destination. Since deviations between the estimated and the real-time traffic conditions are difficult to avoid because of the volatile characteristics that can give rise to delays along the road segments/intersections and at EV battery charging points, each local aggregator runs a real-time congestion control module, as shown on the top right of Figure 1, to deal with the route and charging reservations. Notably, roadside units (RSUs) with computation capability are treated as downstream nodes of a local aggregator to compute the traffic information of nearby road segment(s) or intersection(s) and thereby alleviate the computation loads of local aggregators. Route and charging reservation requests from EVs are first collected by the local aggregator during a short time interval that is adaptively adjusted by the system operator during rush hours. Then, the local aggregator forwards the route and charging reservation requests to RSUs and charging point(s) downstream, respec-

tively. Upon receiving the route reservation requests of EVs, the RSUs and charging point(s) launch a new round of route and charging reservation handling modules, as shown on the bottom right and the bottom left of Figure 1, respectively.

All RSUs and charging points first place the updated reservation requests of EVs into the corresponding reservation queues and compute traffic information and charging costs. The updated traffic conditions and charging costs are forwarded to the local aggregator upstream. After receiving the reply from the local aggregator, each requesting EV checks for any discrepancy in the trip time and charging cost between the EV's earlier estimation and the replied results from the local aggregator upstream. The EV then confirms the reservations with the local aggregator upstream if the trip time and charging cost are within the acceptable range set by the EV. The above-mentioned routing path and charging option selection process iterates until a satisfactory route and charging option are available or all candidate routes are saturated. Different from other approaches in the literature, this work avoids traffic congestion by denying requests from late-booking EVs to traverse through a saturated road segment during rush hours if the traffic density detected at each road segment exceeds a preset threshold. The late-booking EV that receives such a refusal of approval from local aggregator can then delay the departure time until heavy traffic is alleviated, or the EV driver can also take the option of ridesharing/public transportation service instead.

In this work, route reservation(s) and charging request(s) for road segments/intersections and

charging point(s) at distant region(s) will be handled by the remote local aggregator(s). Here we assume each local aggregator also keeps the updated traffic information of the geographical region(s) managed by neighboring local aggregator(s). Accordingly, the EV can obtain the traffic information of surrounding areas from the local aggregator upstream in real time. Since a local aggregator is in charge of the road intersections/segments and the charging points within a geographical region, local aggregators can exchange real-time traffic and charging information of other areas with one other. As for a long driving trip, the neighboring local aggregator(s) can request the real-time traffic and charging information of distant areas for the EV. The traffic and charging information of distant areas is also kept in the database of the requesting local aggregator so that it can be provided if a future request arrives.

In the case where no satisfactory route path is available from the origin to the destination due to traffic control by local aggregators, or if the EV user is not satisfied with a prolonged travel time travel plan, the local aggregator upstream will be requested to find a rideshare service that fits the EV user's needs, as shown in the top middle of Figure 1. If no rideshare is available, public transportation will be suggested instead. Here, it should be noted that the proportions of grants for the reservations of EVs with one, two, or more riders are adjusted dynamically during peak and off-peak hours. The ratios can be adjusted for arterial roads and arterial roads/residential streets as well, subject to the degree of road saturation. Meanwhile, parts of residential streets that connect whole regions of the metropolitan area are free from congestion control so that a late-booking EV is still able to move toward its destination even if it has not been approved to traverse crowded road segments due to the operation of traffic control during rush hours. In the event of no satisfactory route path being found, available scheduled public transportation(s) options are suggested to the EV user instead. Accordingly, possible traffic congestion can be effectively prevented in advance, thereby alleviating drivers' potential inconvenience arising from unexpected extra trip time sitting in traffic jams.

A brief flow chart of the proposed congestion-preventing EV route and charging planning system is illustrated in Figure 2. The detailed descriptions of the above-mentioned modules are given below.

2.1. Route and Charging Planning of an EV

This module is initiated after an EV user sets up a trip plan. An EV user can run this module up to one day in advance of departure to compute the route and charging option before the trip. After the EV moves, this module is executed at every fixed interval— set as fifteen minutes or fewer in this module, to keep track of the updated traffic conditions. The EV first generates a candidate route list and estimates the trip time according to global map data kept in the EV's database. The EV then checks to verify if the traffic information for the segments/intersections and charging information of the charging points over the geographical region(s) between the origin and the destination within the duration of the estimated trip time is available and valid. If it is not, the EV requests the local aggregator upstream to provide missing traffic and charging information.

The local aggregator then estimates the travel time of the vehicle traversing the road segments and intersections by using SVRs. The newly updated time traversed over the road segments/intersections, along with the waiting time and service time at designated charging point(s), are sent to the EV as well. After the most suitable route and charging plan is determined, the EV sends a route and charging reservation request to the local aggregator upstream.

During the computation of the routing path, the EV simultaneously monitors the capacity of its battery, which is the state of charge (SOC), to make sure it can arrive at the destination without depleting the electricity of the battery. Three kinds of charging options are offered in this work, including plug-in charging stations, battery-swapping stations, or certain roads with wireless charging. We assume that the service charge for on-road wireless charging would be the highest because the EV charges while it runs, whereas the charging cost would be the lowest for plug-in charging stations, owing to the fact that the EV needs to spend more time charging. Accordingly, EV users who wish to spend less travel time will choose on-road wireless charging, if possible. In contrast, EV users who consider charging cost to have the highest priority will choose a plug-in charging station as the charging option. If an EV user chooses the plug-in charging option, the EV will get charged at a designated plug-in charging station until the EV battery

Figure 2

Flow chart of the congestion-preventing EV route and charging planning
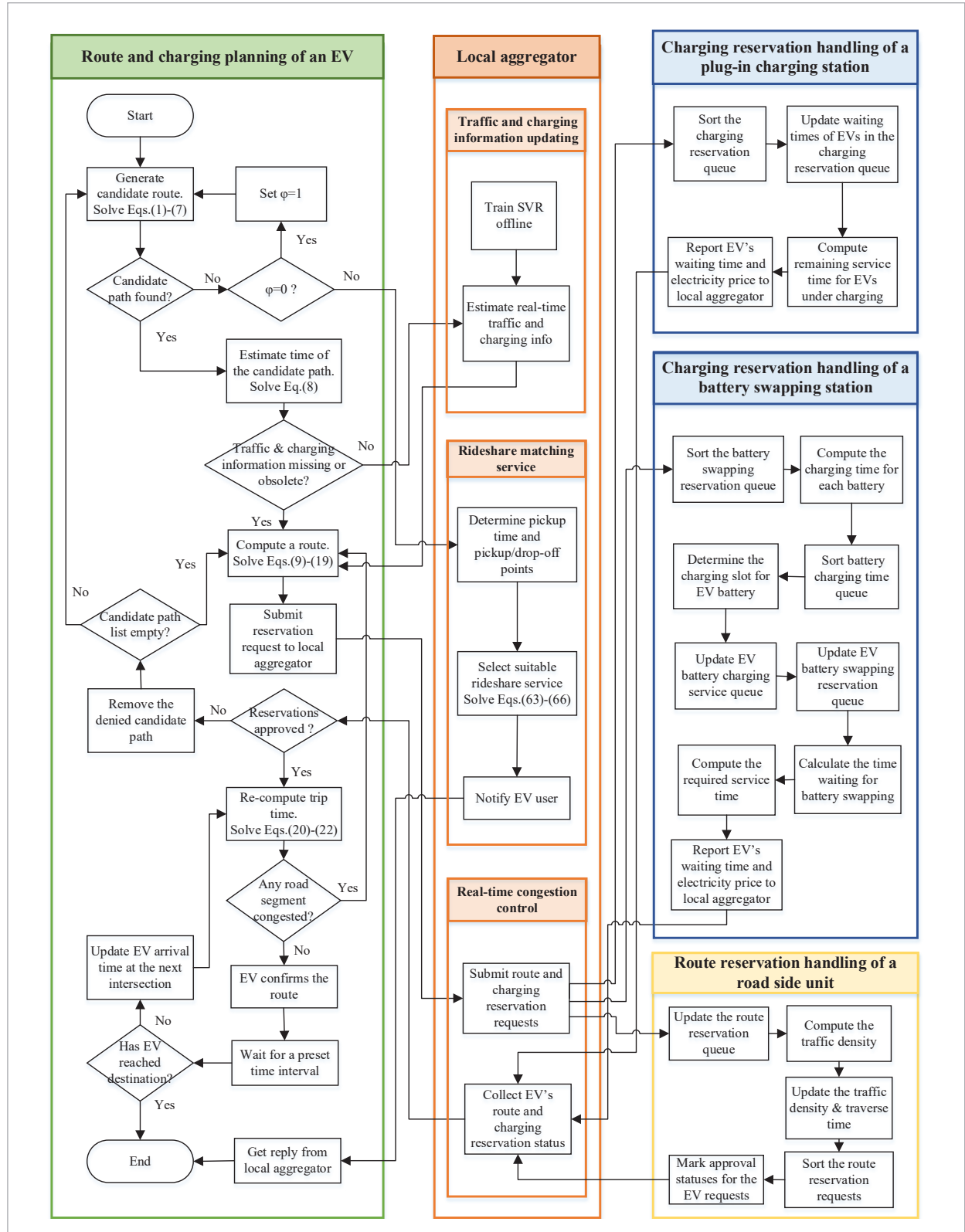
has enough power to reach the destination. In addition, we assume each charging point will announce real-time electricity recharging prices regularly and forward these prices to the local aggregator upstream. Therefore, the EV can update its cache by requesting the local aggregator upstream to provide the announced electricity-recharging price of the candidate charging point(s).

If an EV reservation request is denied by the local aggregator, the EV excludes all the candidate routes that include road segments with traffic densities over and above their preset thresholds during rush hours, and attempts to find an alternative route. On the other hand, the EV confirms the reservations with the local aggregator upstream if the request is granted, so long as the trip time and charging cost fall within the acceptable range set by the EV. The above-mentioned routing path and charging option selection process iterates until the route and the charging point(s) for the EV are found or the road networks are fully saturated. In the latter case of saturated traffic, this module will suggest that the EV user postpones the departure time at the origin or at certain road intersection(s) to avoid traffic jams. However, if a late-booking EV user is still unsatisfied the delayed schedule, the local aggregator upstream will be requested to look for a feasible rideshare solution for the EV driver.

As mentioned earlier, the grant for the reservation of an EV depends upon the number of passengers in the EV. The intention of this traffic control policy is to reduce the number of moving vehicles during rush hours. In addition, this work assumes that most of the EV owners provide rideshare service for others, being motivated to do so by the reward policy provided by the traffic management organization.

The details of this module are presented below:

Step 1: Generate the candidate route list starting from the current location to the destination based on the global road traffic data kept in the EV as follows:

$$\mathbf{D}_{s,e}[j] = \sum_{\gamma l,m \in \{0,1\}} sl_{l,m} l,m, \forall l,m \in \Gamma, \ 0 < j \le K \quad (1)$$

subject to:

$$\mathbf{D}_{s,e}[0] = 0 \quad (2)$$

$$\mathbf{D}_{s,e}[j-1] \le \mathbf{D}_{s,e}[j] \quad (3)$$

$$sl_{l,m} = \infty, \ \forall (l,m) \notin \vartheta \quad (4)$$

$$\sum_{l,m\in\Gamma}\gamma_{l,m} - \sum_{l,m\in\Gamma}\gamma_{l,m} = \begin{cases} 1, & l=s \\ -1, & l=e \\ 0, & \text{otherwise} \end{cases} \quad (5)$$

$$\sum_{\gamma_{l,r}\in\{0,1\}}\gamma_{l,r} \ge 1, \text{if } SOC_{dep} - ac\cdot\mathbf{D}_{s,e}[j] < SOC^{min} \quad (6)$$

$$\sum_{\gamma_{l,q}\in\{0,1\}}\gamma_{l,q} \ge 1, \ \text{if q is a pickup/drop off point}, \quad (7)$$

where $\mathbf{D}_{s,e}[j]$ represents the driving distances for the route indexed by j. s and e stand for the origin and destination locations, respectively. q denotes the pickup/drop off point designated by a rideshare passenger if the EV offers rideshare service. $sl_{l,m}$ stands for the length of the road segment between node l and m. r denotes the index of a charging point, which is treated as a road intersection here. ϑ denotes the set of road segments included in the directed graph, respectively. $\gamma_{l,m}$ is a binary decision variable representing whether the EV traverses over the road segment between nodes l and m. SOC_{dep} denotes the state of charge (SOC) of the EV before departing from the current position, and SOC_{min} represents the lower bound of SOC that should be kept in the EV battery. ac is the average consumption of the EV battery power per kilometer.

Notably, the road map kept by the EV is expressed as a weighted directed graph. Each node of the graph represents a road intersection or a charging point, and each connecting edge stands for the length of the corresponding road segment. If no road segment is found between two nodes, the arc length between the two nodes is set to infinity. Meanwhile, three kinds of charging options are treated as ordinary road segments at this moment for simplicity. In addition, a list expressed as $\mathbf{P}_{s,e}[j] = \left(n_{j,1}, n_{j,2}\right), \left(n_{j,2}, n_{j,3}\right), \cdots, \left(n_{j,u-1}, n_{j,u}\right)$ is associated with all traversed nodes of the jth candidate path. Here $n_{j,i}$ stands for the ith node on the jth path to reach the destination, and u is the number of nodes on the jth path to the destination.

Step 2: Since this module will set the length of the congested road segment to ∞ in the subsequent steps, it is possible that no candidate paths are available during the peak period because the length of the congested road segment is set to ∞. This situation is indicated by setting a flag φ=1 and the second round of path selection will be initiated. In the second round of route selection, this module delays the departure time of the EV at the origin, rest station(s) or road intersection(s) to avoid traffic congestion.

If a suitable candidate path is found at Step 1, continue to Step 3 below. Otherwise, check whether the value of φ is 0. If so, after setting φ=1 and resetting all congested road sections to their road lengths, return to Step 1 to start the second round of path selection. Conversely, when the value of φ has been set to 1, it means that a route that meets the needs of EV users cannot be found during the second round of path selection and charging. At this time, the local aggregator upstream will be asked to find a suitable ride-sharing service for the EV user. If no suitable ride-sharing service is available, the EV user will be advised to take public transportation. This module ends execution here.

Step 3: Estimate the time required for the EV to reach the destination through the longest candidate path, as follows:

$$dat_K = \sum_{1 \le i < u} \left(ait_{n_{K,i}} + ast_{n_{K,i},n_{K,i+1}} \right), \tag{8}$$

where K is the index value of the longest candidate path, u is the number of nodes on the longest candidate path; $ait_{n_{K,i}}$ and $ast_{n_{K,i},n_{K,i+1}}$ represent the average time spent at the road intersection $n_{K,i}$ and the road segment connecting $n_{K,i}$ to $n_{K,i+1}$, respectively.

Step 4: Check if the traffic and charging information is missing or obsolete within the duration of the whole trip. If it is, request the local aggregator upstream to offer the updated traffic and charging information. Notably, if the traversed zones from the current location to the destination are not covered by the local aggregator upstream, the request(s) of traffic and charging information for distant areas can be forwarded by the current local aggregator to neighboring local aggregator(s) until the request(s) are received by the local aggregator(s) that manage the distant area(s). The local aggregator upstream keeps the updated traffic and charging information of other areas in its database after receiving the replies from other local aggregator(s). The updated traffic and charging information of other areas can be used for handling other requests from EVs before a preset deadline.

Step 5: After the updated traffic and charging information is acquired, compute a route that suits the preference of the EV user with designated charging point(s) included if needed:

$$\arg_j \ Min\{\omega_1 \cdot td_j + \omega_2 \cdot (at_{n_{j,u}} - at_{n_{j,1}}) + \omega_3 \cdot$$
$$[\sum_{1 \le i \le u} \phi_{n_{j,i}} \cdot RP_{n_{j,i}}(at_{n_{j,i}}) \cdot cp_{n_{j,i}} \cdot ct_{n_{j,i}} + \sum_{1 \le i < u} \theta_{n_{j,i}} \cdot$$
$$RP_{n_{j,i}}(at_{n_{j,i}}) \cdot cp_{n_{j,i}} \cdot ST_{n_{j,i},n_{j,i+1}}(at_{n_{j,i}}) + \sum_{1 \le i < u} \psi_{n_{j,i}} \cdot$$
$$RP_{n_{j,i}}(at_{n_{j,i}}) \cdot (SOC^{max} - SoC_{n_{j,i}})]\} \tag{9}$$

subject to:

$$td_j = \sum_{i=1}^{u-1} sl_{n_{j,i},n_{j,i+1}} \tag{10}$$

$$at_{n_{j,1}} = t_{dep} \tag{11}$$

$$at_{n_{j,i+1}} = at_{n_{j,i}} + del_{n_{j,i}} + IT_{n_{j,i},n_{j,i+1}}\left(at_{n_{j,i}}\right) +$$
$$ST_{n_{j,i},n_{j,i+1}}\left(at_{n_{j,i}}\right) + \phi_{n_{j,i}} \cdot \left[WT_{n_{j,i}}\left(at_{n_{j,i}}\right) + ct_{n_{j,i}}\right] +$$
$$\psi_{n_{j,i}} \cdot \left[WT_{n_{j,i}}\left(at_{n_{j,i}}\right) + BST_{n_{j,i}}\left(at_{n_{j,i}}\right)\right], 1 \le i < u \tag{12}$$

$$\rho_{n_{j,i},n_{j,i+1}}\left(at_{n_{j,i}}\right) < \rho^{max}_{n_{j,i},n_{j,i+1}}, \text{ if } \varphi = 0 \tag{13}$$

$$del_{n_{j,i}} =$$
$$\begin{cases} \arg \underset{\varepsilon \ge 0}{Min}(\varepsilon), \text{if } = 1 \& \rho_{n_{j,i},n_{j,i+1}}\left(at_{n_{j,i}} + \varepsilon\right) \le \rho^{max}_{n_{j,i},n_{j,i+1}} \\ \qquad 0, \qquad\qquad\qquad \text{Otherwise} \end{cases} \tag{14}$$

$$SoC_{n_{j,1}} = SOC_{dep} \tag{15}$$

$$SoC_{n_{j,i+1}} = SoC_{n_{j,i}} + \eta \cdot \phi_{n_{j,i}} \cdot cp_{n_{j,i}} \cdot ct_{n_{j,i}} +$$
$$\eta \cdot \theta_{n_{j,i}} \cdot cp_{n_{j,i}} \cdot ST_{n_{j,i},n_{j,i+1}}\left(at_{n_{j,i}}\right) + \psi_{n_{j,i}}$$
$$\cdot \left(SOC^{max} - SoC_{n_{j,i}}\right) - ac \cdot SL_{n_{j,i},n_{j,i+1}}, 1 \le i < u \tag{16}$$

$$0 \le ct_{n_{j,i}} \le ct^{max}_{n_{j,i}}, \text{if } \phi_{n_{j,i}} = 1 \tag{17}$$

$$SOC^{min} \le SoC_{n_{j,i}} \le SOC^{max}, 1 \le i \le u \tag{18}$$

$$0 \le \eta \le 1. \tag{19}$$

Three parameters used in Eq. (9) from left to right stand for the total traveling distance of the jth path from the current position of the EV to the destination, the traveling time required for reaching the destination, and the charging costs of the charging point(s), respectively. Three weights ω_1, ω_2, and ω_3 can be pre-

set by the EV user to determine the priorities of the three minimization objectives. Notably, the EV will set ω_3 to zero if no electricity charge is required for the EV before reaching the destination. Here $n_{j,1}$ and $n_{j,u}$ represent the nodes at the current position and at the destination, respectively.

$\phi_{n_{j,i}}$, $\theta_{n_{j,i}}$, and $\psi_{n_{j,i}}$ are binary decision variables that represent whether a plug-in charging station, on-road wireless charging, or a battery swapping station located at node $n_{j,i}$ is chosen for battery recharging for the EV, respectively.

φ stands for a binary flag used by the EV to indicate whether the road network no longer accepts late-booking vehicles owing to traffic saturation during rush hours. φ is initialized to zero the first time this module is run. In the case of traffic saturation, no candidate routes are permitted by the local aggregator upstream. At this moment, φ is set to one and the EV can initiate the second round of route and charging planning by delaying the leaving time at $n_{j,i}$ during rush hours.

$at_{n_{j,i}}$ stands for the EV's arrival timestamp at $n_{j,i}$, $del_{n_{j,i}}$ represents the delayed departure time for the EV at $n_{j,i}$ when traffic saturation occurs at time $at_{n_{j,i}}$. $\rho_{n_{j,i},n_{j,i+1}}(t)$ denotes the traffic density on the road segment between $n_{j,i}$ and $n_{j,i+1}$ at time t, $\rho_{n_{j,i},n_{j,i+1}}^{\max}$ is the upper bound of the traffic density for a road segment between $n_{j,i}$ and $n_{j,i+1}$, and t_{dep} is the timestamp associated with the time when the EV starts moving from the current position.

$sl_{n_{j,i},n_{j,i+1}}$ stands for the length of the road segment between $n_{j,i}$ and $n_{j,i+1}$. $IT_{n_{j,i},n_{j,i+1}}(t)$ represents the delay required for the EV to traverse over the road intersection $n_{j,i}$ that connects $n_{j,i}$ and $n_{j,i+1}$ at time t, and $ST_{n_{j,i},n_{j,i+1}}(t)$ stands for the travel time of the vehicle traversing the segment that connects $n_{j,i}$ and $n_{j,i+1}$ at time t. The derivation of $IT_{n_{j,i},n_{j,i+1}}(t)$ and $ST_{n_{j,i},n_{j,i+1}}(t)$ will be given at the subsequent subsection.

$RP_{n_{j,i}}(t)$ represents the real-time charging electricity price at a charging point $n_{j,i}$ at time t. $cp_{n_{j,i}}$ denotes the charging power per time unit for a plug-in charging station and on-road wireless charging. $ct_{n_{j,i}}^{\max}$ stands for the maximal time that an EV is allowed for charging at a plug-in charging station $n_{j,i}$, whereas $ct_{n_{j,i}}$ denotes the charging time requested by the EV. Notably, $ST_{n_{j,i},n_{j,i+1}}(t)$ is used to represent the charging time for on-road wireless charging as well because the EV

is charged while it moves along the road segment between the starting point of on-road wireless charging $n_{j,i}$ and the end of the on-road wireless charging $n_{j,i+1}$. $WT_{n_{j,i}}(t)$ represents the waiting time for the EV that arrives at a plug-in charging station or battery swapping station. $BST_{n_{j,i}}(t)$ denotes the average EV battery swapping time at a battery swapping station $n_{j,i}$ at time t. Here we assume that $ct_{n_{j,i}}^{\max}$ is kept at the database of the local aggregator upstream. The charging point $n_{j,i}$ reports the real-time charging price $RP_{n_{j,i}}(t)$ along with the latest charging information $WT_{n_{j,i}}(t)$ and $BST_{n_{j,i}}(t)$ to the local aggregator upstream. The derivations of $WT_{n_{j,i}}(t)$ and $RP_{n_{j,i}}(t)$ are given at Sections 2.3 and 2.4.

$SOC^{\max}$ represents the upper bound of the SOC of the EV battery, and $SoC_{n_{j,i}}$ denotes the SOC of the EV battery after the EV arrives at $n_{j,i}$.

Step 6: The EV submits the route and charging reservation request for the selected route to the local aggregator upstream and waits for the reply from the local aggregator, including all updated traffic and charging information within the region governed by the local aggregator.

Step 7: Check the approval status of each traversed road segment/intersection replied from the local aggregator upstream. If all reservations are approved, proceed to Step 9. Otherwise, remove the element(s) of candidate path list $\mathbf{P}_{s,e}$ that include denied road segments or intersections.

Step 8: If $\mathbf{P}_{s,e}$ is not empty, proceed to Step 5 to find an alternative path. Otherwise, proceed to Step 11 in case of empty $\mathbf{P}_{s,e}$.

Step 9: Once the reservation is approved, the EV re-computes the trip time based on the real-time update given by the local aggregator upstream and checks whether the time to arrive at each road intersection of the jth candidate path is earlier than or delayed from the originally estimated off-peak period to the peak period.

$$at_{n_{j,1}}^{new} = at_{n_{j,1}} \tag{20}$$

$$at_{n_{j,i+1}}^{new} = at_{n_{j,i}}^{new} + it_{n_{j,i},n_{j,i+1}} + st_{n_{j,i},n_{j,i+1}} + \phi_{n_{j,i}} \cdot \left(wt_{n_{j,i}} + ct_{n_{j,i}} \right) + \psi_{n_{j,i}} \cdot \left(wt_{n_{j,i}} + bst_{n_{j,i}} \right), 1 \le i < u \tag{21}$$

$$cg_{n_{j,i},n_{j,i+1}} =$$
$$\begin{cases} 1, & \text{if } \rho_{n_{j,i},n_{j,i+1}}\left(at_{n_{j,i}}\right) < \rho_{n_{j,i},n_{j,i+1}}^{gmin} \text{ and} \\ & \rho_{n_{j,i},n_{j,i+1}}^{gmin} \leq \rho_{n_{j,i},n_{j,i+1}}\left(at_{n_{j,i}}^{new}\right) \\ 0, & \text{Otherwise} \end{cases} \quad (22)$$

where $at_{n_{j,i}}^{new}$ represents the updated arrival time at $n_{j,i}$. $it_{n_{j,i},n_{j,i+1}}$ represents the delay time of the EV passing through the road intersection connecting $n_{j,i}$ and $n_{j,i+1}$; $st_{n_{j,i},n_{j,i+1}}$ stands for the travel time of the vehicle traversing the segment or on-road wireless charging that connects $n_{j,i}$ and $n_{j,i+1}$; $wt_{n_{j,i}}$ and $ct_{n_{j,i}}$ stand respectively for the waiting time and the charging time for the EV at a plug-in charging station $n_{j,i}$; whereas $bst_{n_{j,i}}$ is the battery switching time for the EV at an on-road wireless charging. $\rho_{n_{j,i},n_{j,i+1}}^{g\,min}$ denotes the minimum traffic density that indicates an occurrence of traffic congestion. Eq. (22) checks whether the estimated arrival time at $n_{j,i}$, $at_{n_{j,i}}$ is within the off-peak period, and the actual arrival time $at_{n_{j,i}}^{new}$ is in the peak period. If so, it means the deviation of the actual arrival time from the estimated arrival time can cause congestion during peak hours to worsen. Thus, the jth path should be removed from the candidate route list. Here, $cg_{n_{j,i},n_{j,i+1}}$ is marked as 1 to indicate this situation.

Step 10: Check if any road segment(s) of the candidate route is (are) congested:

$$cg_{n_{j,1},n_{j,u}} = \sum_{i=1}^{u-1} cg_{n_{j,i},n_{j,i+1}}. \quad (23)$$

If $cg_{n_{j,1},n_{j,u}} = 0$ and $at_{n_{j,u}}^{new}$ does not exceed the latest arrival time set by the EV user, proceed to Step 12. Otherwise, remove the candidate path $\mathbf{P}_{s,e}[j]$ from $\mathbf{P}_{s,e}$. If there are other candidate paths available, return to Step 5 to find a suitable alternative path.

Step 11: In the event that $\mathbf{P}_{s,e}$ is empty, it indicates that all candidate paths selected in Step 1 are congested. Then the length of all congested road segments of the selected candidate paths are set to ∞, and return to Step 1 to find alternative K candidate paths.

Step 12: At this step, it is implied that a suitable route and charging option has been found. The EV then confirms the route and charging appointment with the local aggregator upstream.

Step 13: Wait for a preset time interval.

Step 14: If the EV has not reached the destination, $at_{n_{j,1}}$ is set to the actual time of arrival at the next road intersection.

Step 15: Proceed to Step 9 to check whether the time to arrive at each road intersection of the jth candidate path is earlier or delayed from the originally estimated off-peak period to the peak period.

2.2. Traffic and Charging Information Updating at a Local Aggregator

As mentioned earlier, an EV will check whether the required traffic and charging information is missing or obsolete before the EV computes a route that suits the preference of the EV user. If any information is missing or obsolete within the estimated trip time span, the local aggregator upstream will receive a request from the EV to provide the lacking information. The computation for the route information is complicated because it is difficult to model the vehicle behaviors due to complicated traffic conditions at the road segments/intersections, variable driving speed, weather conditions, etc. On the other hand, it is straightforward to compute the waiting time and service time for an EV that arrives at a plug-in charging station or battery swapping station owing to the constant charging power per time unit and a fixed battery switching time. Accordingly, the latest charging information obtained from charging points within each geographical region can be used directly for the waiting time and service time of the requesting EV.

Since the computation of the time traversing over a road intersection and segment is much more complicated, we thereby employ support vector regressions (SVRs) in this work to estimate the time traversing over each road intersection and segment from the historical driving data. Five parameters were selected from the collected training sample database to predict the travel time of each road segment and intersection in this work. The input parameters of each road segment include the average speed of the EV arriving at the intersection, weather conditions, day of the week, traffic density, and driving behaviors of EV users. The input parameters of each road intersection include weather conditions, day of the week, traffic density, passenger pick-up/drop-off time, and traffic light waiting time. The prediction of the travel time of EV on each road segment is as follows

$$ST_{l,m}(t) =$$
$$\text{SVR}\left(sp_{l,m}(t), _{l,m}(t), wd_{l,m}(t), wt_{l,m}(t), hb\right)' \tag{24}$$

where $\text{SVR}(\cdot)$ stands for the SVR library, $sp_{l,m}(t)$ represents the average speed of the EV at the road segment between l and m at time t, and $\rho_{l,m}(t)$ stands for the traffic density of the road segment between l and m at time t. $wd_{l,m}(t)$ and $wt_{l,m}(t)$ denote the day of the week and the weather condition at time t, respectively, and hb is the driving behavior of EV users. Notably, with the timestamp provided by the requesting EV, the attribute of "weather condition" at the arrival time can be obtained from a weather forecast website, "the day of the week" at the arrival time can be easily computed, and "traffic density" is assumed to be kept at the historical database that is categorized by the day of the week on an hourly basis. Five driving speed levels are used here to indicate the driving behavior of EV users. In addition, $ST_{l,m}(t)$ is used for computing the charging time for on-road wireless charging as well because the EV is charged while it moves along the road segment between the starting point of on-road wireless charging l and the end point of the on-road wireless charging m.

The prediction of the driving time of the EV at each road intersection is as follows:

$$ST_l(t) = \text{SVR}\left(_l(t), wd_l(t), wt_l(t), pd_l(t), tl_l(t)\right), \tag{25}$$

where $\rho_l(t)$ represents the traffic density at the lth road intersection at time t, and $wd_l(t)$ and $wt_l(t)$ denote the day of the week and the weather condition when the EV arrives at the lth road intersection at time t, respectively. $pd_l(t)$ stands for the average time spent picking up and dropping off riders at the lth intersection. This work assumes that each road intersection can be a passenger pick-up/drop-off point. If no passengers enter or exit the EV at the lth intersection, $pd_l(t)$=0. $tl_l(t)$ is the average waiting time at traffic lights at the lth road intersection. If there is no traffic light at the intersection, $tl_l(t) = 0$. Notably, the training of the SVRs for the road segments, intersection, and on-road wireless charging is carried out offline during the off-peak period to avoid the overloading of a local aggregator.

2.3. Real-Time Congestion Control of a Local Aggregator

During a fixed short interval, which is dynamically tuned by the operator during peak periods and off-peak periods, a local aggregator keeps track of incoming EVs' routes and charging reservation requests, arrival time corrections, or reservation cancellations for each road intersection, road segment or the start point of on-road wireless charging within the governing area of the local aggregator. The local aggregator then forwards the route and charging reservation records for the newly requesting EV at the end of the short time interval to the designated downstream RSUs and plug-in charging/battery swapping station(s), respectively, and initiates a new round of route and charging reservation handling at the corresponding RSUs and plug-in charging/battery swapping station(s).

After receiving the updated route and charging reservation statuses from the RSUs and plug-in charging/battery swapping station(s), the local aggregator updates the traffic and charging information at its database and forwards the real-time updated information to the EVs that submitted the reservation requests and the surrounding local aggregators.

2.4. Charging Reservation Handling of a Plug-In Charging Station

Upon receiving a charging scheduling request from the local aggregator upstream, the plug-in charging station starts a new iteration of this module. Incoming EVs' charging reservations, arrival time corrections, or the cancellation of the charging service reservation are updated in the charging reservation queue. Each record of the charging reservation queue includes three attributes, which are the arrival timestamp, the charging time, and the waiting time of the EV. This module also maintains a service queue for each charging slot that records the time of the EVs receiving the charging service at the corresponding charging slot. Notably, the remaining service time for EVs under charging before the end of the current iteration is kept in the database as a reference for the computation during the next iteration. The waiting time for each EV is computed and forwarded to the EV for reservation confirmation at the end of the current iteration.

The details of this module are presented below:

Step 1: The first element in the service queue for each charging slot is set to the current time plus the remaining service time for the EV under charging at the corresponding charging slot. That is,

$$\mathbf{SQ}_s\left[1\right] = t^{cur} + rst_s, 1 \le s \le \kappa,\tag{26}$$

where κ stands for the number of the charging slots, $\mathbf{SQ}_s$ represents the service queue of the sth charging slot, t^{cur} denotes the current time, and rst_s stands for the remaining service time for the EV under charging at the sth charging slot since the start time of the current iteration. Notably, rst_s was computed before the end of the previous iteration, and rst_s is set to zero during the first time this module is executed.

Step 2: Sort the charging reservation queue in an ascending order based on the arrival time of the EVs revised during the past short time interval specified by the local aggregator upstream.

Step 3: The index of the reservation queue and the index of the service queue for each charging slot are both set to one:

$$w = 1, p_s = 1, \quad 1 \le s \le \kappa,\tag{27}$$

where w denotes the index of the reservation queue, and p_s stands for the index of the service queue for the sth charging slot.

Step 4: Determine the next available charging slot by:

$$ns = \arg_s Min\left(\mathbf{SQ}_s\left[p_s\right]\right), 1 \le s \le \kappa.\tag{28}$$

Step 5: Retrieve the next record form the charging reservation queue. Update the service queue of the chosen charging slot ns, and calculate the waiting time for the EV indexed by w in the reservation queue as follows:

$$\mathbf{RQ}^{wt}\left[w\right] = \begin{cases} \mathbf{SQ}_{ns}\left[p_{ns}\right] - \mathbf{RQ}^{arr}\left[w\right], & \text{if } \mathbf{SQ}_{ns}\left[p_{ns}\right] > \mathbf{RQ}^{arr}\left[w\right] \\ 0, & \text{otherwise} \end{cases}\tag{29}$$

$$\mathbf{SQ}_{ns}\left[p_{ns}+1\right] = \begin{cases} \mathbf{SQ}_{ns}\left[p_{ns}\right] + \mathbf{RQ}^{ct}\left[w\right], & \text{if } \mathbf{SQ}_{ns}\left[p_{ns}\right] > \mathbf{RQ}^{arr}\left[w\right] \\ \mathbf{RQ}^{arr}\left[w\right] + \mathbf{RQ}^{ct}\left[w\right], & \text{otherwise} \end{cases}\tag{30}$$

$$w = w+1, p_{ns} = p_{ns} +1, 1 \le ns \le \kappa\tag{31}$$

where $\mathbf{RQ}^{arr}\left[w\right]$, $\mathbf{RQ}^{ct}\left[w\right]$, and $\mathbf{RQ}^{wt}\left[w\right]$ represent the arrival time, the required charging time, and the waiting time of the EV indexed by the w in the charging reservation queue, respectively.

Repeat Step 4 and Step 5 until all waiting times of EVs in the charging reservation queue are computed.

Step 6: Compute the required service time of the EV under charging service at the start time of the next iteration:

$$\arg_{h_s}\left(\mathbf{SQ}_s\left[h_s\right] \le t^{cur} + < \mathbf{SQ}_s\left[h_s+1\right]\right)\tag{32}$$

$$rst_s = \mathbf{SQ}_s\left[h_s+1\right] - \left(t^{cur} + \Delta\right),\tag{33}$$

where h_s denotes the index of the service queue for the sth charging slot, and Δ stands for the short time interval specified the local aggregator upstream. rst_s is kept in the database for reference during the next iteration.

Step 7: Report the expected waiting time and real-time electricity price for each EV in the charging reservation queue to the local aggregator upstream.

2.5. Charging Reservation Handling of a Battery Swapping Station

Upon receiving a charging scheduling request from the local aggregator upstream, the battery swapping station starts a new iteration of this module. Incoming EVs' charging reservations, arrival time corrections, or the cancellation of the swapping service reservations are revised in the battery swapping reservation queue. Each record of the battery swapping reservation queue includes three attributes, which are the arrival timestamp, the battery switching time, and the waiting time of the EV. Meanwhile, this module establishes three kinds of queues, which include a charging time queue for the batteries that need charging and computes the required charging time for each battery that waits for charging, a battery charging service queue for each charging slot that records the time of each battery starting charging at the corresponding charging slot, and a queue that records the time that an EV battery swapping service is available. Notably, the remaining charging time for the battery under

charging at each charging slot is computed and kept in the database before the end of the current iteration. The waiting time for each EV is then derived and forwarded to the EV for reservation confirmation at the end of the current iteration.

The details of this module are presented below:

Step 1: The first element in the battery charging service queue for each charging slot is set to the start time of the current iteration plus the remaining time for the battery under charging at the corresponding charging slot. That is,

$$\mathbf{BCQ}_c[1] = t^{cur} + rct_c, 1 \le c \le \kappa,\qquad(34)$$

where κ stands for the number of the charging slots, $\mathbf{BCQ}_c$ represents the battery charging service queue, t^{cur} denotes the time the module starts the current iteration, and rct_c stands for the remaining time for the battery under charging at the sth charging slot since the start time of the current iteration. Notably, rct_c was computed at the previous epoch and rct_c is set to zero the first time this module is executed.

Step 2: Sort the battery swapping reservation queue in an ascending order based on the arrival times of the EVs collected during the past Δ time interval.

Step 3: Compute the charging time for each battery that will be waiting for charging by:

$$\mathbf{CT}[b] = \frac{SOC^{b,max} - SOC^b_{cur}}{cp}, 1 \le b \le \alpha,\qquad(35)$$

where α is the number of the batteries waiting for recharging, $\mathbf{BCT}[b]$ denotes the charging time for the battery indexed by b, and cp represents the charging power per time unit for the battery swapping station. $SOC^{b,max}$ represents the upper bound of the SOC for the bth battery, whereas SOC^b_{cur} denotes the SOC for the bth battery after being swapped.

Step 4: Sort **BCT** in an ascending order based on the time required for the batteries to be fully charged.

Step 5: The indices of **BCT** and $\mathbf{BCQ}_c$ are all set to ones:

$$b = 1, p_c = 1, 1 \le c \le \kappa,\qquad(36)$$

where b represents the index of **BCT** and p_c stands for the index of $\mathbf{BCQ}_c$.

Step 6: Determine the charging slot for the battery with the least battery charging time:

$$nc = \arg_c Min\left(\mathbf{BCQ}_c[p_c]\right), 1 \le c \le \kappa.\qquad(37)$$

Step 7: Retrieve the required charging time from the next record from the sorted **BCT**, and update the battery charging service queue of the selected charging slot nc as follows:

$$\mathbf{BCQ}_{nc}[p_{nc}+1] = \mathbf{BCQ}_{nc}[p_{nc}] + \mathbf{BCT}[b],\qquad(38)$$

$$b = b+1, p_{nc} = p_{nc}+1, \ 1 \le nc \le \kappa\qquad(39)$$

Repeat Step 6 and Step 7 until $b > \alpha$.

Step 8: The index of the available EV battery swapping service queue is set to one,

$$s = 1.\qquad(40)$$

Step 9: If σ batteries are already fully charged at the start time of the current iteration, assign the σ batteries into the available EV battery swapping queue. If $\sigma \le \pi$,

$$\mathbf{ESQ}[s] = t^{cur}, s = s+1, 1 \le s \le \sigma.\qquad(41)$$

Otherwise, it indicates that the number of the fully charged batteries is larger than that of the parallel swapping services. Then the fully charged batteries are assigned as follows:

$$\mathbf{ESQ}[s] = t^{cur} + \varsigma \cdot t^{sw}, s = s+1,$$
$$(\varsigma-1)\pi \le s \le \min(\sigma, \varsigma\pi)\qquad(42)$$

where π stands for the number of available parallel battery swapping services, ς is a positive integer, and t^{sw} denotes the battery switching time.

Step 10: The indices of $\mathbf{BCQ}_c$ are all set to ones. That is,

$$p_c = 1, 1 \le c \le \kappa.\qquad(43)$$

Step 11: Determine the next charging slot with the earliest time of charging completion by,

$$nc = \arg_c Min\left(\mathbf{BCQ}_c[p_c]\right), 1 \le c \le \kappa.\qquad(44)$$

Step 12: Insert the next record into **ESQ** as follows:

$$\mathbf{ESQ}[s] = \mathbf{BCQ}_{nc}[p_{nc}] \tag{45}$$

$$s = s+1, p_{ns} = p_{ns}+1, 1 \le ns \le \kappa \tag{46}$$

Repeat Step 11 and Step 12 until $s > \sigma + \alpha$.

Step 13: The index of the battery swapping reservation queue and that of the available EV battery swapping service queue are both set to one:

$$w = 1, s = 1, \tag{47}$$

where w denotes the index of the battery swapping reservation queue and s stands for that of the available EV battery swapping service queue.

Step 14: Retrieve the next record from the battery swapping reservation queue, and calculate the waiting time for the EV that needs battery-swapping service as follows:

$$\mathbf{SRQ}^{wt}[w] = \begin{cases} \mathbf{ESQ}[s] - \mathbf{SRQ}^{arr}[w], & \text{if } \mathbf{ESQ}[s] > \mathbf{SRQ}^{arr}[w] \\ 0, & \text{otherwise} \end{cases} \tag{48}$$

$$\mathbf{SRQ}^{sw}[w] = t^{sw} \tag{49}$$

$$w = w+1, s = s+1, 1 \le s \le \kappa, \tag{50}$$

where $\mathbf{SRQ}^{arr}[w]$, $\mathbf{SRQ}^{sw}[w]$, and $\mathbf{SRQ}^{wt}[w]$ represent the arrival time, the required battery switching time, and the waiting time of the EV indexed by the w in the battery swapping reservation queue.

Repeat this step until all waiting times of EVs in the battery swapping reservation queue are computed.

Step 15: Compute the required service time of each battery under charging service at the start time of the next iteration:

$$\arg_{h_c} \left(\mathbf{BCQ}_c[h_c] \le t^{cur} + \Delta < \mathbf{BCQ}_c[h_c+1] \right) \tag{51}$$

$$rct_c = \mathbf{BCQ}_c[h_c+1] - (t^{cur} + \Delta), \tag{52}$$

where h_c denotes the index of the battery charging service queue for the cth charging slot. rct_c is kept in the database for reference during the next iteration.

Step 16: Report the computed waiting time and real-time electricity price to each EV on the battery swapping reservation queue to the local aggregator upstream.

2.6. Route Reservation Handling of a Road Side Unit

Upon receiving the route reservation handling request from the local aggregator upstream, a sorted route reservation queue in ascending order based on arrival times of EVs is revised. The RSU counts the number of EVs on the road segment/intersection, estimates the traverse times, and updates the traffic density of the road segment/intersection for the requesting EVs. As mentioned earlier, the grant for an EV reservation depends upon the number of passengers in the EV. The proportions of grants for the reservations of EVs with one, two, or more riders are adjusted dynamically during peak and off-peak hours. The ratios are adjusted for arterial roads and circumferential roads/residential streets as well, subject to the degree of road saturation. Notably, EVs moving toward different directions on a road segment or intersection are separately counted for the corresponding traffic densities. The updated traffic information is replied to the local aggregator upstream at the end of the current iteration.

The details of this module are presented below:

Step 1: Update the route reservation queue for each road segment and intersection governed by the RSU in ascending order based on the arrival times of EVs. Each record of the route reservation queue includes the arrival timestamp of a requesting EV, the time that the EV issued the reservation request, the traffic density at the arrival time, the traverse time and approval status of the corresponding road segment or intersection.

Step 2: Initialize the variables needed during the computation of the traffic density of the road segment/intersection:

$$u_{l,m}^0 = 1, \tau_{l,m} = \mathbf{ATQ}_{l,m}[1], \tag{53}$$

where $\mathbf{ATQ}_{l,m}[1]$ stands for the arrival time of the EV at the first element in the sorted route reservation queue for the road segment between l and m. Notably, the variables for a road intersection l can be defined likewise.

Step 3: Compute the traffic density of the road segment between l and m based on the arrival times of EVs:

$$\underset{u_{l,m}^1}{\arg}\left(\mathbf{ATQ}_{l,m}\left[u_{l,m}^1\right] < \tau_{l,m} + 1 \le \mathbf{ATQ}_{l,m}\left[u_{l,m}^1 + 1\right]\right) \quad (54)$$

$$\rho_{l,m}\left(\tau_{l,m}\right) = \min\left(u_{l,m}^1 - u_{l,m}^0 + 1, \rho_{l,m}^{max}\right), \quad (55)$$

where $\rho_{l,m}\left(\tau_{l,m}\right)$ stands for the traffic density of the road segment that connects l and m between the time $\tau_{l,m}$ and $\tau_{l,m} + 1$, and $\rho_{l,m}^{max}$ denotes the maximal traffic density set for a road segment that connects l and m.

Step 4: Update the traffic density and traverse time of the road segment:

$$\mathbf{TDQ}_{l,m}^{\tau_{l,m}}\left[\varpi\right] = \rho_{l,m}\left(\tau_{l,m}\right), 1 \le \varpi \le (u_{l,m}^1 - u_{l,m}^0 + 1) \quad (56)$$

$$\mathbf{TTQ}_{l,m}^{\tau_{l,m}}\left[\varpi\right] = \mathrm{SVR}\left(\cdot\right), 1 \le \varpi \le (u_{l,m}^1 - u_{l,m}^0 + 1) \quad (57)$$

where $\mathbf{TDQ}_{l,m}^{\tau_{l,m}}\left[\varpi\right]$ and $\mathbf{TTQ}_{l,m}^{\tau_{l,m}}\left[\varpi\right]$ represent the traffic density and traverse time of the ϖ th element in the route reservation queue, respectively. $\mathbf{TTQ}_{l,m}^{\tau_{l,m}}$ is used as an update for the traverse time computed at Section 2.2. A unique $\mathrm{SVR}\left(\cdot\right)$ is used to estimate the traverse time for a road segment between l and m after training with the dataset. Notably, the computation for a road intersection is identical to that for a road segment except that the notation $\rho_l(\cdot)$ is used to represent the traffic density at the road intersection l.

Step 5: Sort the $(u_{l,m}^1 - u_{l,m}^0 + 1)$ elements between $\mathbf{ATQ}_{l,m}\left[u_{l,m}^0\right]$ and $\mathbf{ATQ}_{l,m}\left[u_{l,m}^1\right]$ based on the order in which the EVs issued the reservation requests, and assign the $(u_{l,m}^1 - u_{l,m}^0 + 1)$ EV requests to separate queues with different numbers of EV passengers. Three queues that correspond with one, two, or more passengers, denoted as $\mathbf{ASQ}_{l,m}^{\tau_{l,m},1}$, $\mathbf{ASQ}_{l,m}^{\tau_{l,m},2}$, and $\mathbf{ASQ}_{l,m}^{\tau_{l,m},3}$, respectively, are established in this module.

Step 6: Mark approval statuses for the $(u_{l,m}^1 - u_{l,m}^0 + 1)$ EV requests as follows.

$$\mathbf{ASQ}_{l,m}^{\tau_{l,m},np}\left[\mu\right] = \begin{cases} 1, & \text{if } 1 \le \mu \le \rho_{l,m}^{np,max} \\ 0, & \text{otherwise} \end{cases} \quad (58)$$

$$\rho_{l,m}^{max} = \rho_{l,m}^{1,max} + \rho_{l,m}^{2,max} + \rho_{l,m}^{3,max}, \quad (59)$$

where $\mathbf{ASQ}_{l,m}^{\tau_{l,m},np}\left[\mu\right]$ represents the approval status

of the μth EV in the queue $\mathbf{ASQ}_{l,m}^{\tau_{l,m},np}$. The value of np are 1, 2, or 3. $\rho_{l,m}^{np,max}$ denotes the maximal number of EVs with np passengers allowed to traverse through the road segment that connects l and m. Here $\mathbf{ASQ}_{l,m}^{\tau_{l,m},np}\left[\mu\right]$ is set to one if the reservation of the μth EV is approved. Otherwise, it is set to zero. In other words, no more reservations for an EV with np passengers is granted if the number of the requesting EVs in the queue $\mathbf{ASQ}_{l,m}^{\tau_{l,m},np}$ reaches a preset threshold $\rho_{l,m}^{np,max}$.

Step 7: Update the variables $u_{l,m}^0$ and $\tau_{l,m}$:

$$u_{l,m}^0 = u_{l,m}^1, \tau_{l,m} = \tau_{l,m} + 1 \quad (60)$$

Proceed to Step 3 until the traffic density is set for the road segment connecting l and m, and approval statuses are marked for the EVs in the route reservation queue.

Step 8: Reply with the traffic densities and approval statuses of the reserved road segments/intersections to the local aggregator upstream.

2.7. Rideshare Matching Service Provided by a Local Aggregator

Since the late-booking EV users are not allowed to drive their private EVs through crowded road segments with traffic control during rush hours, this work assumes that the government formulates some traffic control policy to offer an incentive or bonus to EV owners so that they are encouraged to offer rideshare service to others who need a ride with an acceptable fare. Accordingly, this work also provides a rideshare matching service so those who are not able to drive their private EVs can still reach their destinations on time during rush hours.

Once it receives a late-booking EV user's rideshare matching request, the local aggregator upstream first computes the desirable pickup and drop off points, which are road intersections close to the origin and destination. Then the local aggregator selects the most appropriate route for the late-booking EV user.

The details of this module are presented below:

Step 1: The local aggregator selects the candidate pickup and drop off points that are close to the origin and the destination of a rideshare passenger:

$$\underset{p}{\arg}\left|\left(x_s,y_s\right)-\left(x_p,y_p\right)\right|\leq d_s^{max} \qquad (61)$$

$$\underset{d}{\arg}\left|\left(x_e,y_e\right)-\left(x_d,y_d\right)\right|\leq d_e^{max}, \qquad (62)$$

where $\left(x_s,y_s\right),\left(x_e,y_e\right),\left(x_p,y_p\right)$, and $\left(x_d,y_d\right)$ stand for the coordinates of the origin, the destination, the pth pickup, and dth drop off point, respectively. d_s^{max} represents the maximal distance between the origin and the pickup point, whereas d_e^{max} is the maximal distance between the destination and the drop off point that can be acceptable by the rideshare passenger.

Step 2: Use an available tool such as Google Maps to determine the time at which the rideshare passenger will reach the candidate pickup point from the origin at the designated departure time.

Step 3: Assume that a path expressed as $P_v=\left(n_{v,1},n_{v,2}\right),$ $\left(n_{v,2},n_{v,3}\right),\cdots,\left(n_{v,u-1},n_{v,u}\right)$ stands for the route of the EV indexed by v. Select the most suitable rideshare service by:

$$\underset{v,k,l}{\arg}Min\{v_1\cdot[\,|\,(x_s,y_s)-(x_{n_{v,k}},y_{n_{v,k}})\,|+$$
$$|\,(x_e,y_e)-(x_{n_{v,k}},y_{n_{v,k}})\,|\,]+v_2\cdot(at_{n_{v,l}}-at_{n_{v,k}})+ \qquad (63)$$
$$v_3\cdot rp_v\}$$

subject to:

$$n_{v,k}=p\,,\ n_{v,l}=d \qquad (64)$$

$$at_{n_{v,k}}\geq t_s^{dep}+wt\left(s,n_{v,k}\right) \qquad (65)$$

$$NR_v<NR_v^{max}, \qquad (66)$$

where v_1, v_2, and v_3 represent three weights that can be preset by the rideshare passenger to determine the priorities of the three minimization objectives. $n_{v,k}$ and $n_{v,l}$ stand for two road intersections traversed by the vth EV, where the two road intersections are candidate pickup point p and drop off point d of the rideshare passenger. Three minimization objectives in Eq. (63) from left to right stand for the walking distance from the origin to the pickup point plus that from the drop off point to the destination, the traveling time required from the pickup point to the drop off destination, and rideshare fare, respectively. $at_{n_{v,k}}$ denotes the arrival time of the EV at the pick-up point $n_{v,k}$, whereas t_s^{dep} is the departure time of the rideshare passenger from the origin. $wt\left(s,n_{v,k}\right)$ represents the time that the rideshare passenger takes when she/he walks from the origin to the pick-up point $n_{v,k}$. NR_v and NR_v^{max} stand for the current number of riders in the EV and the seating capacity of the EV, respectively.

Step 4: If a rideshare service is available for the ride passenger, notify the ride passenger and the EV that provides the rideshare service.

3. Case Study and Numerical Experiments

We evaluated the performance of the proposed work by applying it to the downtown area and its surrounding neighborhoods in a metropolitan city in Taiwan. A series of simulations were run to examine whether the proposed work is effective for solving the traffic congestion problem faced by the aforementioned metropolitan city.

3.1. Experimental Settings

The presented framework was coded in version 3.8 of Python. Simulations were performed on a PC with Intel Core i7 at 4.1 GHz CPU, and 12GB RAM. The historical driving data were obtained from a real-time traffic information web site of Taichung City, Taiwan [21]. The retrieved information from the database includes average speed and traffic density detected at the entrance of a road segment every five minutes. Based on the retrieved traffic density and average speed, we generated 173,093 records for all EVs within a day, where the attributes for each record include the average speed of the EV at the road segment, the traffic density of the road segment, the day of the week, the weather conditions, and the driving behavior of each EV user. The speed of the EV was obtained by randomly adding/deducting a value within the range -10% to +10% from the average speed detected at the road segment every five minutes. Since driving behaviors of EV users are not available in the dataset, they were postulated based on the speed profiles given above. Five driving speed levels were set here for all EVs to reflect the driving behaviors of EV users.

The investigated road segments include three arterial roads, four circumferential roads, and fifteen residen-

tial streets. The lengths of the first and the second arterial roads are shorter than that of the third arterial road, and the third arterial road is parallel to the first and the second arterial roads. The residents living in the surroundings of the first and the second arterial roads can take whichever arterial road is the closest as their route to the destination. Meanwhile, the concatenation of the first and the second arterial roads can be adopted as an alternative route to the third arterial road. We assume that a battery swapping station is located at both of the first and the second arterial roads, and on-road wireless charging is available on the third arterial road. The traditional plug-in charging stations are distributed along the circumferential roads and residential streets. The battery switching time is set to 3 minutes [6] and the charging time at a plug-in charging station is set to 30 minutes [8].

Uniform distribution is employed for generating the origin and the destination of each EV within the geographical distribution of road segments. The time spent for picking up and dropping off riders at a road intersection is set between 15 and 30 seconds, depending on the number of riders; and the waiting time at a traffic light at a road intersection is set between 0 and the duration of the period of the traffic light turning from red to green.

There are four stages in the simulations. At the first stage, we evaluate the prediction accuracy of SVRs for the estimation of the traverse time over each road segment collected from the database. Next, we examine the performance of the proposed congestion control mechanism. At the third stage, we apply the rideshare matching service in conjunction with the congestion control and evaluate the outcomes. At the last stage of the simulations, we contrast the performance of

the proposed strategies with that of a representative congestion-mitigation algorithm that appears in the recent literature [16], in which a strategy of route reservations with travel time predictions is used to tackle the traffic congestion problem. The detailed descriptions of the separate stages of the simulations are given below.

3.2. Off-line Prediction Analysis

At the first stage of the simulations, we examine the prediction accuracy of SVRs for the estimation of the traverse time over each road segment. The prediction accuracy is measured by the Mean Absolute Relative Error (MARE) and Mean Square Error (MSE) methods. The MARE can be expressed by,

$$\text{MARE} = \frac{1}{n}\sum_{i=1}^{n}\frac{|a_i - b_i|}{a_i}, \tag{67}$$

where a_i and b_i denote the prediction and estimated results, respectively.

The MSE can be expressed by,

$$\text{MSE} = \frac{1}{n}\sum_{i=1}^{n}\left(a_i - b_i\right)^2, \tag{68}$$

where a_i and b_i denote the prediction and estimated results, respectively. A lower MARE percentage and a lower MSE indicates higher prediction accuracy, and vice versa.

Table 1 shows the comparison of SVR predictions before and after adding the attribute of driving behavior of each EV user. It can be seen that the prediction accuracy is substantially improved after one original parameter of the SVRs, the average EV speed detect-

Table 1

Comparison of prediction error for average traverse times of road segments before and after adding the attribute of EV users' driving behavior

Road type	Traverse time	MSE (before)	MSE (after)	MARE (before)	MARE (after)
Arterial road 1	205.3 (sec)	5.18 (sec)	2.81 (sec)	12.61%	7.05%
Arterial road 2	325.4 (sec)	6.40 (sec)	1.73 (sec)	14.71%	6.81%
Arterial road 3	415.7 (sec)	16.00 (sec)	0.92 (sec)	13.83%	4.52%
Circumferential roads	527.5 (sec)	10.61 (sec)	1.48 (sec)	19.31%	12.49%
Residential streets	179.2 (sec)	8.32 (sec)	1.66 (sec)	23.02%	13.63%

ed at the entrance of each road segment, is replaced by the speed of each specific EV when entering a road segment. Accordingly, the prediction of the traverse time of each road segment with the amended database provides reliable estimation of the trip time from the origin of the EV to its destination. Notably, since estimation errors might cause an EV to become stuck in a traffic jam in some cases, this problem is dealt with in the route and charging planning module, as illustrated in Section 2.1.

3.3. Outcomes of the Proposed Congestion Control Mechanism

Figure 3 illustrates the average travel and charging times of EVs on different types of road segments before the congestion control mechanism was activated. It can be observed from Fig. 3 that the average travel time of each arterial road segment rose significantly due to the increase in traffic. It is assumed that most EV drivers prefer to choose a path that takes a shorter time and incurs less charge waiting time, and on-road wireless charging on the third arterial road fits the needs of this kind of EV driver. As a result, without traffic control, the traffic flow during the peak periods exceeded the capacity of all arterial roads and caused congestion. The situation was even worse at the third arterial road, which provides on-road wireless charging. Notably, only one-way traffic is investigated in this work due to the fact that only traffic moving toward one direction was collected in the dataset. It can be seen that the commuters driving to work during the peak period in the morning resulted in the heaviest traffic within a day.

Figure 3

Illustration of average travel and charging times of EVs on different types of road segments before congestion control
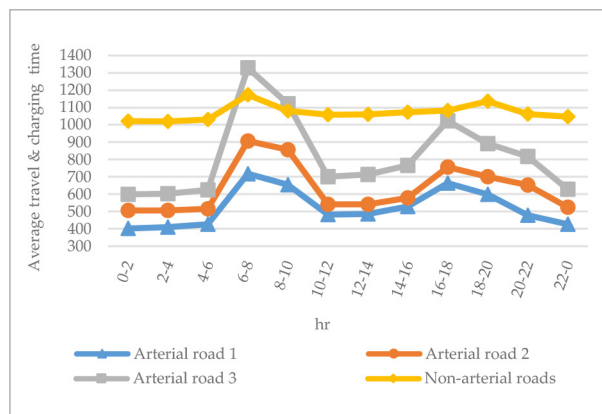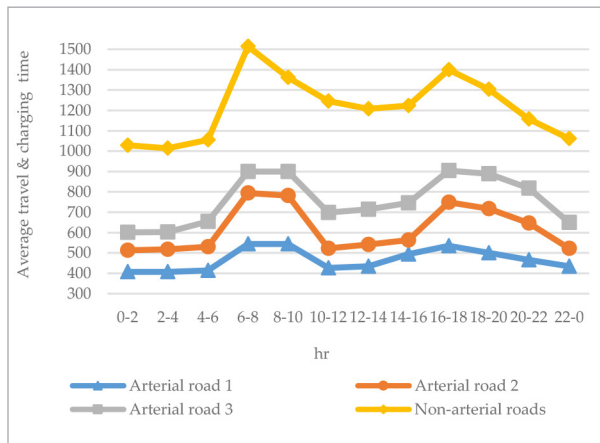

Figure 4 shows the traffic flow distribution of EVs on the three arterial roads and circumferential roads/residential streets before congestion control. Most EV drivers prefer taking the arterial roads owing to shorter driving time and charging time. This is the reason why the percentage of EVs taking the arterial roads, especially the third arterial road that provides on-road wireless charging service, increases significantly when the traffic flow increases, and the gap is even larger during rush hours. In contrast, the traffic on circumferential roads and residential streets was relatively smooth during the peak periods.

Figure 4

Traffic flow distribution of EVs before congestion control
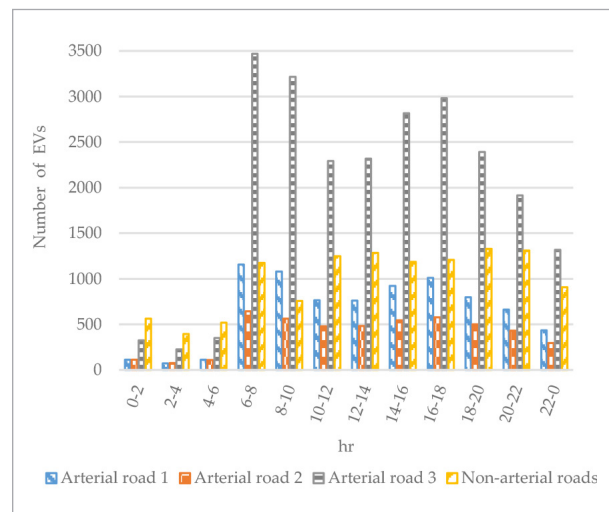
Recalling that the preferences of EV users are considered in this work, it can be assumed that most EV users still wish to arrive at their destination on time, even during the rush hours. After observing travel times and the flow distribution on all road segments as illustrated in Figs. 3-4, and considering that the capacity of each arterial road is affected by the road length, we activated the reservation policy for each arterial road before depature of the EVs. Once an arterial road has reached the maximal capacity, no more EVs are allowed to traverse the arterial road. If an EV cannot travel on the arterial road(s), the EV driver will be advised to divert to the circumferential roads or residential streets, while taking into account the charging requirements of the EV driver. Recall that only plug-in charging stations are deployed on

circumferential roads/residential streets in this work. Accordingly, an EV driver demanding low-cost charging will take circumferential roads/residential streets instead of the faster arterial roads. It can be observed from Fig. 5 that the average travel and charge times of EVs increase significantly on circumferential roads/residential streets during rush hours owing to the high number of vehicles, even though the traffic flow on each arterial road is well controlled.

Figure 5
Illustration of average travel and charging times of EVs on different types of road segments after congestion control

Figure 6 shows the traffic flow distribution of EVs on the three arterial roads and circumferential roads/residential streets after congestion control. The traffic flow of each arterial road is limited via the realization of the reservation policy in the proposed traffic control mechanism. Late-booking EV drivers were not allowed to rush into the arterial road(s) for shortening driving time or charging waiting time. Thus, the EVs driving on the arterial roads did not encounter congestion and had their demand for short charging time met. Nevertheless, late-booking EV drivers were diverted to the low-speed circumferential roads/residential streets, while some EV drivers took the option of postponing their departure time to the off-peak period. It can be concluded that the increase of the extra time an EV spent for driving and charging during the peak periods and the diversion of traffic flow due to the traffic control at the arterial road are two main causes for the significant increase of the average travel and charge times of EVs on circumferential roads/residential streets during heavier traffic periods.

Figure 6
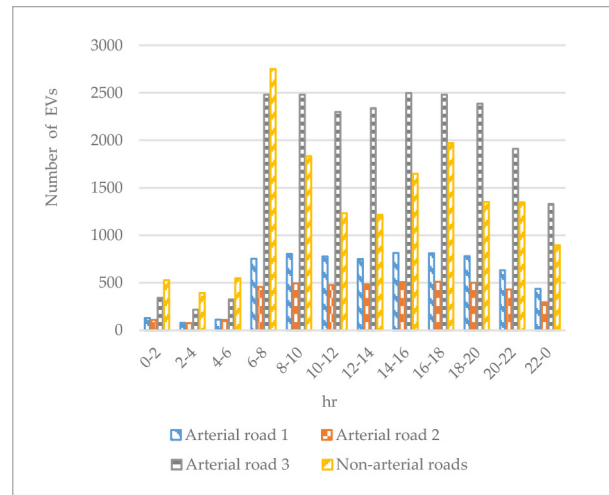Traffic flow distribution of EVs after congestion control

Figure 7 shows the comparison of average travel and charging times of EV drivers that took one or more of the three arterial roads to the destination before and after congestion control. It can be observed that the average travel and charging times rise significantly during rush hours owing to the high number of vehicles if no congestion control is applied. On the other hand, after the congestion control, the average travel and charging times have significantly decreased during the peak periods because the traffic flows of the three arterial roads are well controlled.

Figure 7
Comparison of average travel and charging times of EVs that took the circumferential roads and residential streets before and after congestion control
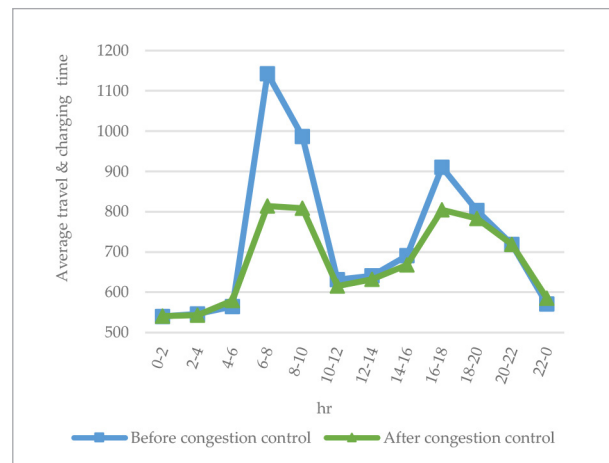
Figure 8 shows the comparison of average travel and charging times of EV drivers that did not take any of the three arterial roads to the destination before and after congestion control. As expected, most of the EV drivers that preferred taking arterial road(s) were forced to take the alternative low-speed circumferential roads/residential streets due to the effect of traffic control. Accordingly, the average travel and charging times on each arterial road only increases slightly during the peak periods after congestion control is applied. However, the average travel and charging time for the EVs that made use of circumferential roads/residential streets increased significantly owing to the surge of the diverted traffic flows.

Figure 8

Comparison of average travel and charging times of EVs that took the circumferential roads and residential streets before and after congestion control
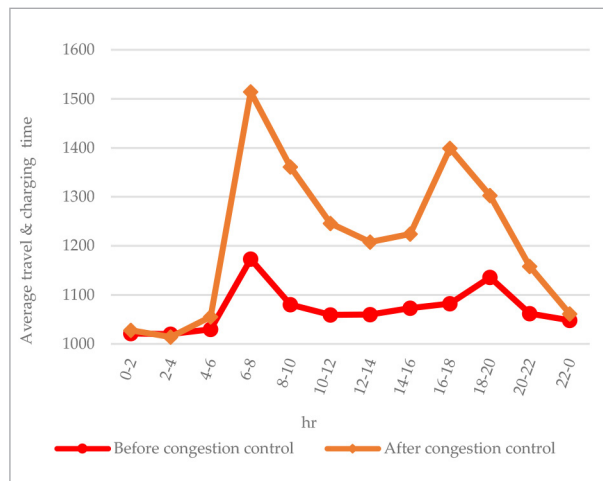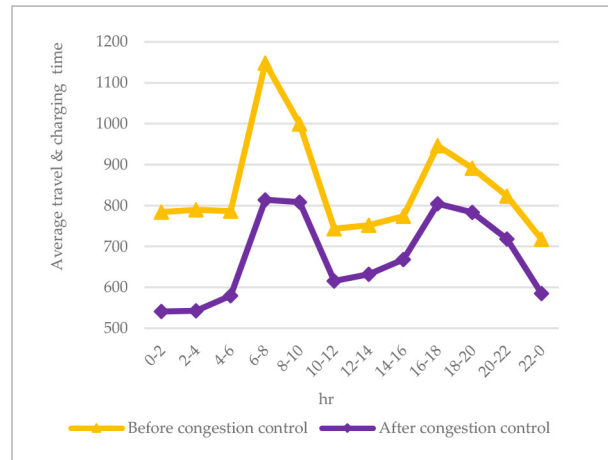

Figure 9 shows the average travel and charging times for the EVs with a time-saving preference before and after congestion control. Recall that this work attempts to find a path with the lowest travel and charging time for an EV driver setting a time-saving preference in the route and charging planning module. Accordingly, the traffic flow is directed into the fast-charging arterial roads or slow-charging circumferential roads/residential streets based on the preference set by each EV driver. Without congestion control, the average travel and charging times rise sharply for all the EVs driving on the arterial roads during the peak period, no matter what the preference set by the EV user is. In contrast, the EV drivers with the short-

est travel and charging time preference can make use of arterial roads until the road capacity is saturated. In addition, a small proportion of the drivers can even delay their departure times to the off-peak period to avoid the increase of travel time owing to the speed limits of circumferential roads/residential streets.

Figure 9

Comparison of average travel and charging times for EVs with a time-saving preference before and after congestion control

3.4. Outcomes of the Proposed Congestion Control Mechanism Plus Rideshare Matching Service

Figure 10 shows the average travel and charging times for the EVs after applying congestion control mechanism plus rideshare matching service. Compared to the average travel and charging times as given in Fig. 5, the average travel and charging time for the EVs driving on the second and the third arterial roads was significantly reduced, and the surges of traffic flow on circumferential roads/residential streets were significantly improved during the peak period. It can be inferred that the reduction of the number of EVs after applying the rideshare matching service contributes to the remarkable improvement of the average travel and charging times for the EVs.

Figure 11 shows the traffic flow distribution on the three arterial roads and circumferential roads/residential streets after applying congestion control and rideshare matching service. Compared to the traffic flow distribution as given in Fig. 6, the number of EVs was significantly reduced after the option of rideshare

Figure 10

Illustration of average travel and charging times of EVs on different types of road segments after applying congestion control mechanism plus rideshare matching service
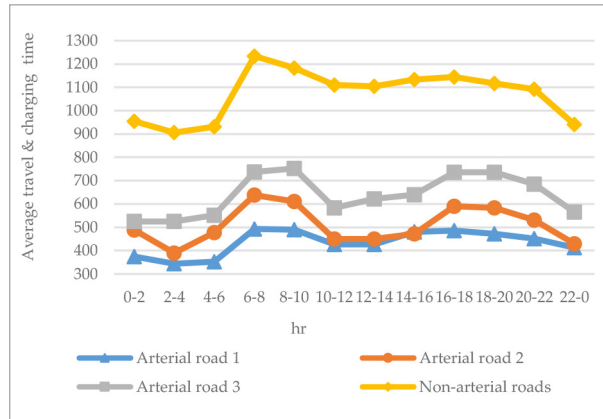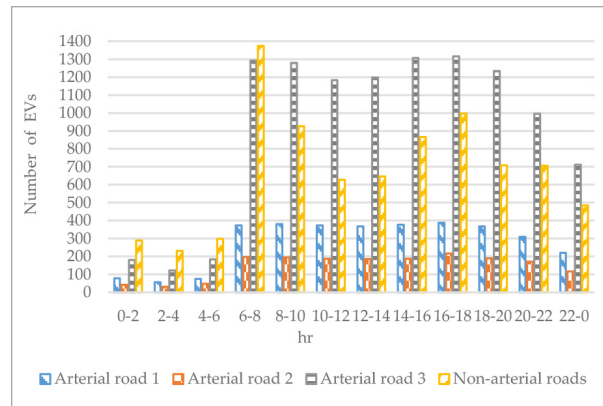

Figure 11

Traffic flow distribution of EVs after applying congestion control and rideshare matching.

services was offered, as shown in Fig. 11. Notably, the number of EVs driving on the third arterial road was higher than the number driving on other types of road segments, as expected, because the third arterial road provides the fastest route and on-road wireless charging service for EV drivers who set a time-saving preference, resulting in riders reducing the time spent on their trips.

3.5. Comparison with a Representative Congestion Control Algorithm

Next, we contrast the performance of three algorithms, including the proposed congestion control mechanism (GC), proposed congestion control plus

rideshare matching mechanisms (GC+RM), and a representative congestion mitigation algorithm from the recent literature (RRTT) [16]. It can be seen from Fig. 12 that the performance of the RRTT algorithm was slightly worse than that of the proposed congestion control mechanism because the vehicle reservation cancellations were not considered in the RRTT algorithm. Meanwhile, early and late vehicle arrivals at the road segments caused by prediction errors also weakened the congestion control effect of the RRTT algorithm. Last but not least, the individual preference of each EV driver was not considered in the RRTT. The proposed rideshare matching approach achieved better performance than that of applying the congestion control alone. The faster driving speed of each EV can be achieved by the decrease of traffic flows. Thus, the average travel and charging time for an EV rider was significantly reduced, even though EV riders needed to wait at the pick-up points before the EVs arrived.

Figure 12

Comparison of average travel and charging times of EV users for three algorithm
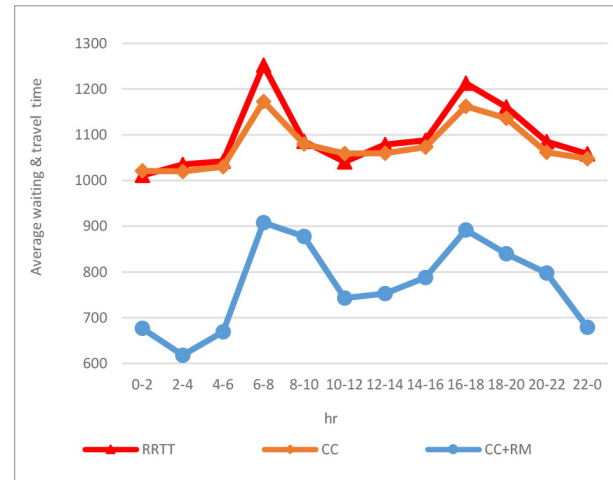
4. Conclusion

It can be observed from the recent literature that little research work has presented congestion-preventing route and charging planning mechanisms for EVs. This research bridges the gap and proposes a congestion control mechanism to deal with the volatile traffic congestion problem in real-time. The proposed

work first estimates the traverse time of each road segment and intersection by using SVRs. Then each EV makes route and charging reservations before departure and keeps the real-time charging information updated after it moves. The traffic is regulated during rush hours by allocating an elastic range to the traveling period for late-booking EVs or offering the EV user the option(s) to take a rideshare service or public transportation. The simulation results reveal that the proposed work can satisfy the preferred route and charging demand(s) of EVs and alleviate traffic congestion effectively.

Acknowledgement

References

1. Ahmad, F., Mahmud, S. A, Yousaf, F. Z. Shortest Processing Time Scheduling to Reduce Traffic Congestion in Dense Urban Areas. IEEE Transactions on Systems, Man, and Cybernetics: Systems, 2017, 47(5), 838-855. https://doi.org/10.1109/TSMC.2016.2521838

2. Angelelli, E., Morandi, V., Speranza, M. G. (2019). A Trade-off Between Average and Maximum Arc Congestion Minimization in Traffic Assignment with User Constraints. Computers and Operations Research, 2019, 110, 88-100. https://doi.org/10.1016/j.cor.2019.05.028

3. Bi, X., Tang, W. K. Logistical Planning for Electric Vehicles Under Time-dependent Stochastic Traffic. IEEE Transactions on Intelligent Transportation Systems, 2018, 20(10), 3771-3781. https://doi.org/10.1109/TITS.2018.2883791

4. Cao, Z., Jiang, S., Zhang, J., Guo, H. A Unified Framework for Vehicle Rerouting and Traffic Light Control to Reduce Traffic Congestion. IEEE Transactions on Intelligent Transportation Systems, 2017, 18(7), 1958-1973. https://doi.org/10.1109/TITS.2016.2613997

5. Gan, X., Zhang, H., Hang, G., Qin, Z., Jin, H. Fast-Charging Station Deployment Considering Elastic Demand. IEEE Transactions on Transportation Electrification, 2020, 6(1), 158-169. https://doi.org/10.1109/TTE.2020.2964141

6. Global EV Battery Swapping Market is Driven by Low Penetration of DC Fast Charging Station and Remunerative Prospects for Shared E-Mobility Services: P and S Intelligence, 2020. https://www.globenewswire.com/news-release/2020/03/19/2003424/0/en/Global-EV-Battery-Swapping-Market-is-Driven-by-Low-Penetration-of-DC-Fast-Charging-Station-and-Remunerative-Prospects-for-Shared-E-Mobility-Services-P-S-Intelligence.html

7. He, J., Yang, H., Tang, T. Q., Huang, H. J. Optimal Deployment of Wireless Charging Lanes Considering Their Adverse Effect on Road Capacity. Transportation Research Part C: Emerging Technologies, 2020, 111, 171-184. https://doi.org/10.1016/j.trc.2019.12.012

8. How Long Does It Take to Charge an Electric Car? 2018. https://pod-point.com/guides/driver/how-long-to-charge-an-electric-car.

9. Ke, J., Yang, H., Zheng, Z. On Ride-Pooling and Traffic Congestion. Transportation Research Part B: Methodological, 2020, 142, 213-231. https://doi.org/10.1016/j.trb.2020.10.003

10. Kim, G., Ong, Y. S., Cheong, T., Tan, P. S. Solving the Dynamic Vehicle Routing Problem Under Traffic Congestion. IEEE Transactions on Intelligent Transportation Systems, 2016, 17(8), 2367-2380. https://doi.org/10.1109/TITS.2016.2521779

11. Kumar, N., Rahman, S. S., Dhakad, N. Fuzzy Inference Enabled Deep Reinforcement Learning-Based Traffic Light Control for Intelligent Transportation System. To appear in IEEE Transactions on Intelligent Transportation Systems, 2020. https://doi.org/10.1109/TITS.2020.2984033

12. Langenberg, T., Lüddecke, T., Wörgötter, F. Deep Metadata Fusion for Traffic Light to Lane Assignment. IEEE Robotics and Automation Letters, 4(2), 2019, 973-980. https://doi.org/10.1109/LRA.2019.2893446

13. Li, Z., Liu, P., Xu, C., Duan, H., Wang, W. Reinforcement Learning-based Variable Speed Limit Control Strategy to Reduce Traffic Congestion at Freeway Recurrent Bottlenecks. IEEE Transactions on Intelligent Transportation Systems, 2017, 18(11), 3204-3217. https://doi.org/10.25148/etd.FI14110778

14. Liang, X., Du, X., Wang, G., Han, Z. A Deep Reinforcement Learning Network for Traffic Light Cycle Control. IEEE Transactions on Vehicular Technology, 68(2), 2019, 1243-1253. https://doi.org/10.1109/TVT.2018.2890726

15. Liu, C., Zhou, M., Wu, J., Long, C., Wang, Y. Electric Vehicles En-Route Charging Navigation Systems: Joint Charging and Routing Optimization. IEEE Transactions on Control Systems Technology, 2019, 27(2), 906-914. https://doi.org/10.1109/TCST.2017.2773520

16. Menelaou, C., Timotheou, S., Kolios, P., Panayiotou, C. G., Polycarpou, M. M. Minimizing Traffic Congestion Through Continuous-time Route Reservations with Travel Time Predictions. IEEE Transactions on Intelligent Vehicles, 2019, 4(1), 141-153. https://doi.org/10.1109/TIV.2018.2886684

17. Pan, J. S., Popa, I. S., Borcea, C. Divert: A Distributed Vehicular Traffic Re-routing System for Congestion Avoidance. IEEE Transactions on Mobile Computing, 2017, 16(1), 58-72. https://doi.org/10.1109/TMC.2016.2538226

18. Ruch, C., Richards, S., Frazzoli, E. The Value of Coordination in One-Way Mobility-on-Demand Systems. IEEE Transactions on Network Science and Engineering, 2020, 7(3), 1170-1181. https://doi.org/10.1109/TNSE.2019.2912078

19. Shi, X., Xu, Y., Guo, Q., Sun, H., Gu, W. A Distributed EV Navigation Strategy Considering the Interaction Between Power System and Traffic Network. IEEE Transactions on Smart Grid, 2020, 11(4), 3545-3557. https://doi.org/10.1109/TSG.2020.2965568

20. Sun, G., Li, G., Xia, S., Shahidehpour, M., Lu, X., Chan, K. W. ALADIN-Based Coordinated Operation of Power Distribution and Traffic Networks with Electric Vehicles. IEEE Transactions on Industry Applications, 2020, 56(5), 5944-5954. https://doi.org/10.1109/TIA.2020.2990887

21. Taichung City Real-time Traffic Information [Online]. http://e-traffic.taichung.gov.tw/RoadGrid/Pages/VD/History2.html

22. Tang, X., Bi, S., Zhang, Y. J. A. Distributed Routing and Charging Scheduling Optimization for Internet of Electric Vehicles. IEEE Internet of Things Journal, 2018, 6(1), 136-148. https://doi.org/10.1109/JIOT.2018.2876004

23. Wang, S., Djahel, S., Zhang, Z., McManis, J. Next Road Rerouting: A Multiagent System for Mitigating Unexpected Urban Traffic Congestion. IEEE Transactions on Intelligent Transportation Systems, 2016, 17(10), 2888-2899. https://doi.org/10.1109/TITS.2016.2531425

24. Wu, C. H., Ho, J. M., Lee, D. T. Travel-time Prediction with Support Vector Regression. IEEE Transactions on Intelligent Transportation Systems, 2004, 5(4), 276-281. https://doi.org/10.1109/TITS.2004.837813

25. Xia, F., Chen, H., Chen, L., Qin, X. A Hierarchical Navigation Strategy of EV Fast Charging Based on Dynamic Scene. IEEE Access, 2019, 7, 29173-29184. https://doi.org/10.1109/ACCESS.2019.2899265

26. Zhang, X., Cao, Y., Peng, L., Ahmad, N., Xu, L. Towards Efficient Battery Swapping Service Operation under Battery Heterogeneity. IEEE Transactions on Vehicular Technology, 2020, 69(6), 6107-6118. https://doi.org/10.1109/TVT.2020.2989195